ACS OMEGA

http://pubs.acs.org/journal/acsodf

Article

Spectroscopic, Electrochemical, and Biological Assays of Copper-Binding Molecules for Screening of Different Drugs and Plant Extracts against Neurodegenerative Disorders

David Brinvillier, Melissa Barrast, Petra Couderc-Murillo, José Bono-Yagüe, Alain Rousteau, Ana Pilar Gómez Escribano, Marcos V. Palmeira-Mello, Antonio Doménech-Carbó, Nady Passe-Coutrin, Muriel Sylvestre, Rafael P. Vázquez-Manrique,* and Gerardo Cebrián-Torrejón*

Cite This: *ACS Omega* 2022, 7, 16260−16269

Read Online

ACCESS | Metrics & More | Article Recommendations

ABSTRACT: Neurodegenerative disorders, caused by prone-to-aggregation proteins, such as Alzheimer disease or Huntington disease, share other traits such as disrupted homeostasis of essential metal ions, like copper. In this context, in an attempt to identify Cu^{2+} chelating agents, we study several organic compounds (ethylenediaminetetraacetic acid, phenylenediamine, metformin, salicylate, and trehalose) and organic extracts obtained from *Bacopa monnieri* L., which has been used in Ayurvedic therapies and presented a broad spectrum of biological properties. For this purpose, UV−visible spectroscopy analysis and electrochemical measurements were performed. Further, biological assays were performed in *Caenorhabditis elegans* models of polyQ toxicity, in an attempt to obtain better insights on neurodegenerative disorders.

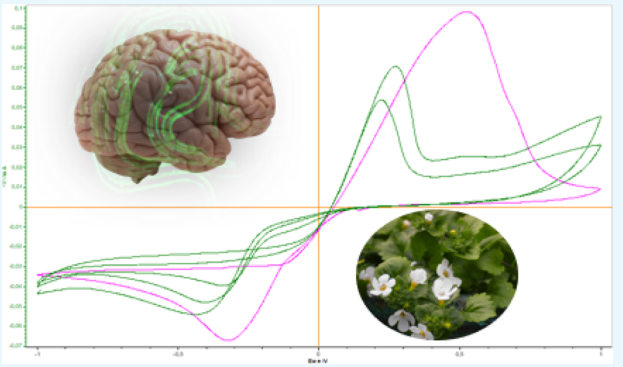

INTRODUCTION

Huntington disease (HD) is a genetic neurodegenerative disorder characterized by uncoordination and choreic movements, progressive loss of cognitive functions, and psychiatric alterations, leading to repercussions in daily life activities.[1] HD is characterized by intracellular deposits of mutant huntingtin (mHttt), which is an essential protein in mammals but with no clear function yet.[2,3] Huntingtin is encoded by *HTT*, and patients of HD have an abnormal expansion of CAG triplets (36 or more) in the first exon of the gene. Hence, mHtt contains an expansion of polyglutamines (polyQs) in its N-terminal region, which makes it very prone to aggregation, and confers it a toxic gain-of-function. Although the mechanism of aggregation is not fully understood, several therapeutic strategies are being studied.[2,3] The present research focuses on the limitation of the aggregation of polyQ-containing peptides and its toxicity, which is attributed to the presence of oligomeric and fibrillary forms. The literature shows that certain metal ions, such as Cu^{2+} and Fe^{2+}, accumulate within mHtt-affected cells and that at least copper contributes to mHtt aggregation.[4] The brain tightly regulates the homeostasis of many metals, such as Cu^{2+}, Zn^{2+}, and Fe^{2+}, as part of normal physiological processes.[5] Copper is a redox transition metal which plays a crucial role in several biological systems.[6] Copper-based complexes have been studied as attractive biological agents,[7] since they may present relevant pharmacological properties and interact with many different biomolecules.[8−10] In the context of neurodegenerative disorders, copper is capable of modulating the aggregation of mutant huntingtin.[4] Additionally, Cu^{2+} can be reduced to Cu^{+}, which in turn is essential for the generation of reactive oxygen species (ROS) via Fenton-like reaction ($Cu^{+} + H_2O_2 \rightarrow Cu^{2+} + OH^{\bullet} + OH^{-}$), thus contributing to oxidative stress, which is extremely important to HD.[2,11,12] Although HD is purely hereditary, current therapies against these neurodegenerative diseases are insufficient to stop the progression of the pathology. In this context, it is increasingly urgent to develop therapies based on the combination of molecules that can act on several aspects of the disease. Moreover, strategies based on medicinal plants have gained attention for the treatment of different neurological diseases.[13−16] Several studies involving polyphenols and their metal chelating properties have been reported.[17,18] Although focused on Alzheimer's disease (AD),

Received: June 29, 2021
Accepted: December 31, 2021
Published: May 4, 2022

they may apply to many other neurodegenerative diseases, whose progression parallels with the aggregation of prone-to-aggregation molecules, such as HD (mutant huntingtin) or Parkinson's disease (α-synuclein). In this regard, Picciano and Vaden[19] investigated the complexation between curcumin and copper(II) ions using different segments of the β-amyloid peptide, one of the molecules causative of AD. The authors concluded that curcumin can simultaneously bind to Cu^{2+} and β-amyloid, forming a ternary system. Recently, similar results were also obtained by Kola and co-workers using rosmarinic acid,[20] and the system was characterized via different spectroscopic techniques. Cytotoxic studies revealed that the copper(II) complex was able to reduce the percentage of cellular viability on NIH3T3 fibroblasts cells. The coordination of these compounds on the copper center can enhance its pharmacological properties, which in turn allows easy crossing of the brain blood barrier by these compounds. Thus, considering the metal chelating property of different natural compounds, an extract from*Bacopa monnieri* L. was used to develop an innovative method for screening anti-neurodegenerative agents using spectroscopic and electrochemical techniques. For this screening, several compounds were selected following two criteria: (i) the potential as chelating agents rich in electron donor atoms (mimicking the chelating properties of the natural products present in Bacopa extracts) and (ii) the neuroprotective bioactivity. *B. monnieri* has been extensively used in neuromedicine, and it has also been shown to present many biological properties.[21] Bacoside A is suggested as the most active constituent on *B. monnieri*, which is used in Ayurvedic therapies for the treatment of several disorders.[22,23] In this work, we describe the study of different organic compounds, including the extracts from *B. monnieri*, as a potential anti-neurodegenerative therapy. Since copper-based complexes can present enhanced pharmacological properties in comparison to the organic-free ligand, the chelation effect may play an important role on neurodegenerative diseases. In this context, UV−vis and cyclic voltammetry techniques were employed to obtain more insights on this feature. Furthermore, due the complexity of the vertebrate brain, two*C. elegans* models of polyQ toxicity were used to investigate the *B. monnieri* effects on neurodegenerative disorders. The analyses showed that *B. monnieri* extracts reduce polyQ aggregation and reduce neurodegeneration induced by these molecules.

RESULTS AND DISCUSSION

Chelation Test via UV−Vis Spectroscopy. UV−vis spectroscopy was employed to investigate the production of copper-based complexes upon addition of extracts of *B. monnieri* (Figure 2A) and different ligands L [L = EDTA, PPD, MET, SAL, TRE (Figure 2B)]. The influence of concentration of MET, SAL, and TRE on $CuSO_4$ λ_{max} is shown in Figure 2B. Although a slight displacement of λ_{max} from 818 to 808 nm was observed after increasing the concentration of MET, there is no evidence regarding the formation of the copper complex. A similar behavior was observed for TRE, with a displacement from 818 to 797 nm. By increasing the amount of SAL in the $CuSO_4$ solution, we noticed a shift in λ_{max}, which decreased from 818 to 790 nm, accompanied by a change of color from blue to light green. Since salicylate presents a chemical structure that can coordinate via the bidentate mode on the metal center,[33] the results suggest a possible formation of the copper complex.

Figure 1. Images of Bacopa plants, which corresponds to the *B. monnieri* L species analyzed in this work (photo was taken by the authors).

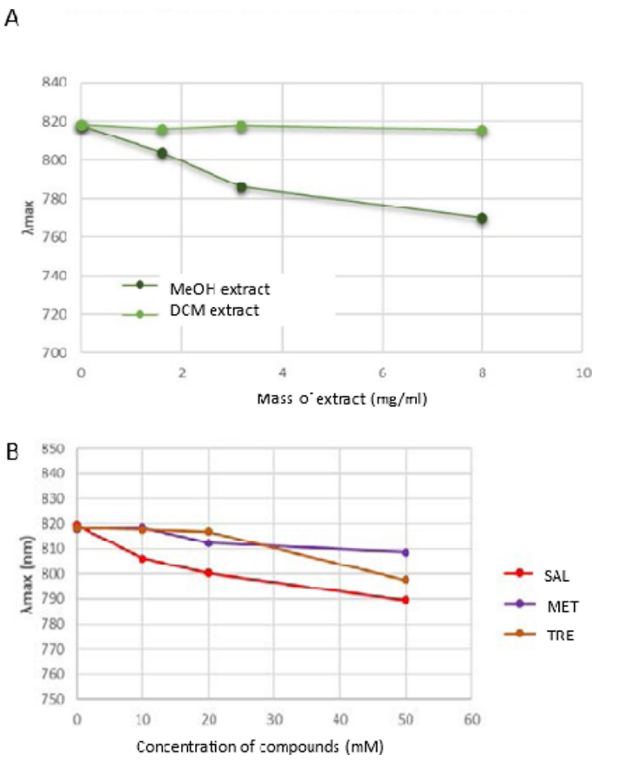

Figure 2. Influence of concentration of (A) extracts of *B. monnieri* (DCM and MeOH) and (B) MET, SAL, and TRE on λ_{max} of $CuSO_4$ 50 mM solution.

Hypsochromic and hyperchromic displacements on λ_{max} of $CuSO_4$ were observed when the amounts of EDTA were increased. The λ_{max} of $CuSO_4$ also decreases in the presence of PPD. In this case, the absorption centered on 810 nm undergoes a hypsochromic displacement toward shorter wavelengths, around 600 nm. It should be mentioned that the solution of PPD 40 mM did not allow us to determine the λ_{max} of $CuSO_4$ due the lack of resolution of the peak. Moreover, the DCM extract does not seem to induce a shift on $CuSO_4$ λ_{max}, which remains close to 818 nm. As observed in Figure 2B, unlike DCM, the MeOH extract induces a displacement from 818 to 770 nm on $CuSO_4$ λ_{max}. Since MeOH is a coordinating solvent,[34] these results suggest the formation of a copper complex.

Chelation Test via Cyclic Voltammetry. As observed in Figure 3, the addition of MET and TRE causes a similar profile on the $CuSO_4$ voltamogram. Peak reduction attributed to the

https://doi.org/10.1021/acsomega.1c03378
ACS Omega 2022, 7, 16260−16269

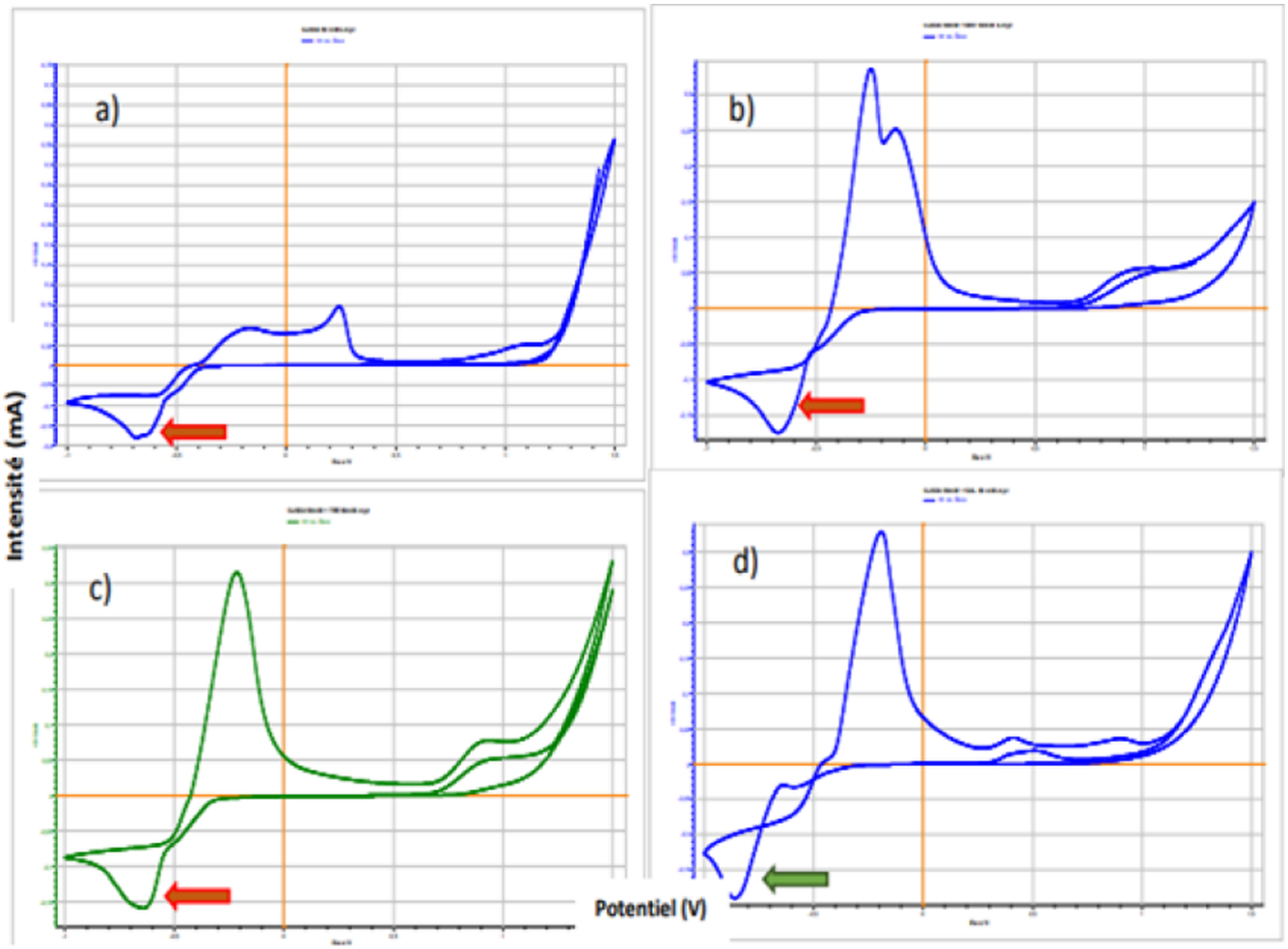

Figure 3. Cyclic voltammograms of solutions of (a) $CuSO_4$ [50 mM], (b) $CuSO_4$ [50 mM] + MET [50 mM], (c) $CuSO_4$ [50 mM] + TRE [50 mM], and (d) $CuSO_4$ [50 mM] + SAL [50 mM] in phosphate buffer 0.10 M, pH 7.0. Potential scan rate: 20 mV s^{-1}.

Cu^{2+} + 2e → Cu^0 process is observed at −0.65 V versus Ag/AgCl (Figure 3a), which is in agreement with the literature data for copper electrochemistry in the presence of weakly complexing agents.[35] In the subsequent anodic scan, the deposit of solid copper is oxidized to Cu^{2+} in solution giving rise to the stripping of oxidation peak at +0.20 V exhibiting peak splitting. This feature can be attributed to the formation of different deposits of metallic copper during the precedent cathodic step, a situation favored by the high Cu^{2+} concentration used in these experiments. The cathodic signal is very similar to that observed when MET and TRE are added in the solution (Figure 3b,c), suggesting no evidence of coordination of these ligands. A different voltammogram was obtained after SAL addition. In this case, the reduction peak was observed at more negative potentials (−0.85 V vs Ag/AgCl) accompanied by a crossover in the following anodic scan. These features are indicative of the coordination of the Cu^{2+} ion with SAL (Figure 3d). The electrochemical results are in agreement with those obtained via UV−vis spectroscopy, and SAL seems to be an effective chelating ligand.

This voltammetric response to Cu^{2+} complexation is in principle equivalent to that observed with EDTA at pH 7.0, as illustrated in Figure 4. In a solution of $CuSO_4$, the reduction of Cu^{2+} to Cu^0 gives a peak at −0.65 V versus Ag/AgCl (Figure 4a). In this region of potentials, EDTA remains electrochemically silent (Figure 4b), only showing overlapping oxidation peaks at ca. 1.0 V, associated to the oxidation of carboxylate units. In 50 mM $CuSO_4$ plus 50 mM EDTA solution (Figure 4c), the cathodic process for Cu^{2+} reduction is negatively shifted to −0.87 while the stripping Cu^0 to Cu^{2+} oxidation collapses to a unique sharp peak at −0.35 V. Similarly, the carboxylate oxidation processes define a unique, broad anodic wave. Further addition of EDTA (Figure 4d) leads to an ill-defined voltammetric response, probably as a result of the overlapping of the Cu^{2+} reduction with the hydrogen evolution reaction. The voltammograms in Figure 5 suggest a complexation between PPD and Cu^{2+}; again, a cathodic shift was observed in the Cu^{2+} reduction wave. However, since PPD is a non-chelating ligand, it is suggested that the formation of the copper−EDTA complex is favored due to the chelation effect in comparison to the copper−PPD complex.

No significant alteration on the Cu^{2+} reduction peak was observed on the $CuSO_4$ voltammogram after the addition of MeOH extracts of *B. monnieri* at 1.16 mg/mL (not shown) and 3.19 mg/mL (Figure 6a). However, a cathodic shift to −0.85 V versus Ag/AgCl was observed with an extract concentration of 7.98 mg/mL, indicating that the concentration is an important feature on this interaction with the metal ion (Figure 6b). The DCM extract of *B. monnieri* at 1.16 mg/mL (not shown) also does not induce a change in the peak Cu^{2+} reduction. As before, there is a significant change in the Cu^{2+} reduction signal at higher extract concentrations (Figure 6d). In contrast

https://doi.org/10.1021/acsomega.1c03378
ACS Omega 2022, 7, 16260−16269

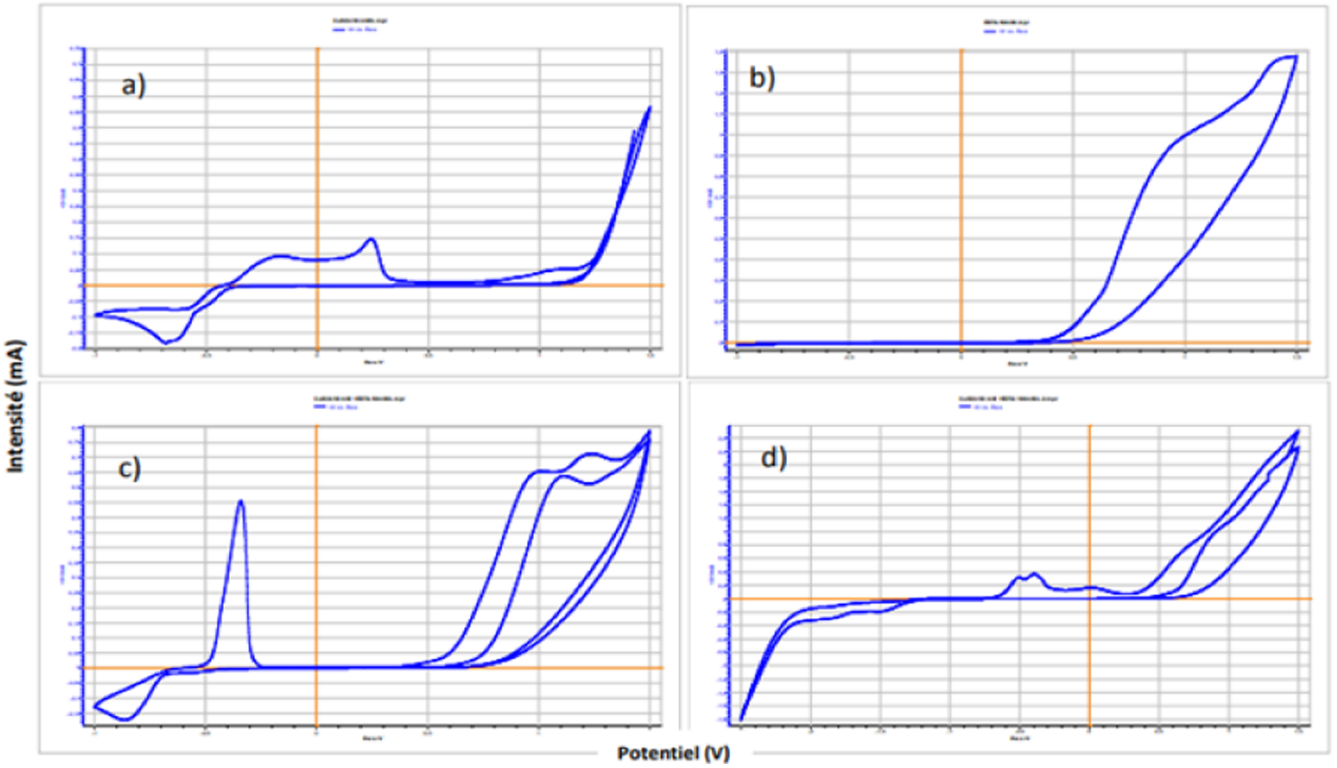

Figure 4. Cyclic voltammograms of solutions of (a) $CuSO_4$ [50 mM], (b) EDTA [50 mM], (c) $CuSO_4$ [50 mM] + EDTA [50 mM], and (d) $CuSO_4$ [50 mM] + EDTA [100 mM] in phosphate buffer 0.10 M, pH 7.0. Potential scan rate: 20 mV s^{-1}.

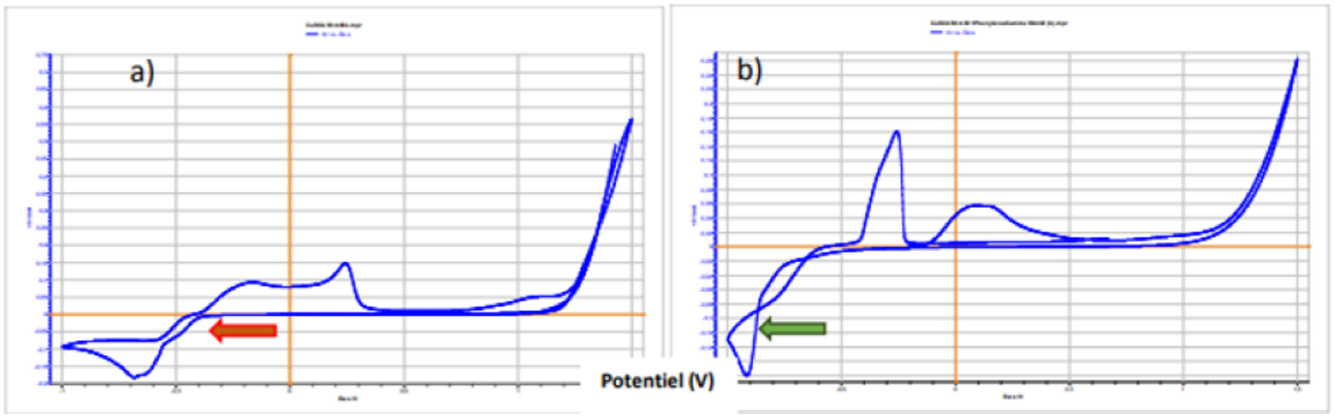

Figure 5. Cyclic voltammograms of solutions of (a) $CuSO_4$ [50 mM] and (b) $CuSO_4$ [50 mM] + PPD [50 mM] in phosphate buffer 0.10 M, pH 7.0. Potential scan rate: 20 mV s^{-1}.

with UV−vis spectra, which do not show an auxochrome effect on copper sulfate in these cases, voltammetric data become sensitive to Cu^{2+} complexation. In this context, the cyclic voltammetry technique will allow us to learn more about the chelating effect of our *B. monnieri* extracts. Additional experiments will be performed in an attempt to obtain more insight on its chelating properties.

Study of Aggregation of PolyQs in *C. elegans*. Bacopa extracts are believed to be neuroprotective in different models of neurodegenerative diseases, such as Alzheimer disease or aluminum-induced neurodegeneration in rats.[36,37] Therefore, we sought to test whether these effects may be relevant in invertebrate models of polyQ aggregation, which recapitulates some events produced in HD,[25,32] a disease which has associated heavy oxidative stress as it also happens in other neurodegenerative disorders.[2,38] To do so, we used the round nematode worm *C. elegans*.[29] This has been used extensively to test genes and signaling pathways that are neuroprotective[30,39,40] and also to test neuroprotective compounds.[25,32] We used two different models of polyQ toxicity: one which expresses 40 glutamines (40Q) fused in a frame with the fluorescent protein YFP in the body wall muscles[30] and another which expresses 112Q in the touch receptor neurons.[25] Analysis of the first model permits investigation of the potential of a substance to reduce polyQ aggregation very easily, since aggregation of the 40Q::YFP can be followed easily under a dissecting microscope equipped with fluorescence. It has been described that mutant huntingtin aggregation, which carries a polyQ expansion of 36 or more glutamines, runs in parallel with the progression of HD.[41] The

https://doi.org/10.1021/acsomega.1c03378
ACS Omega 2022, 7, 16260−16269

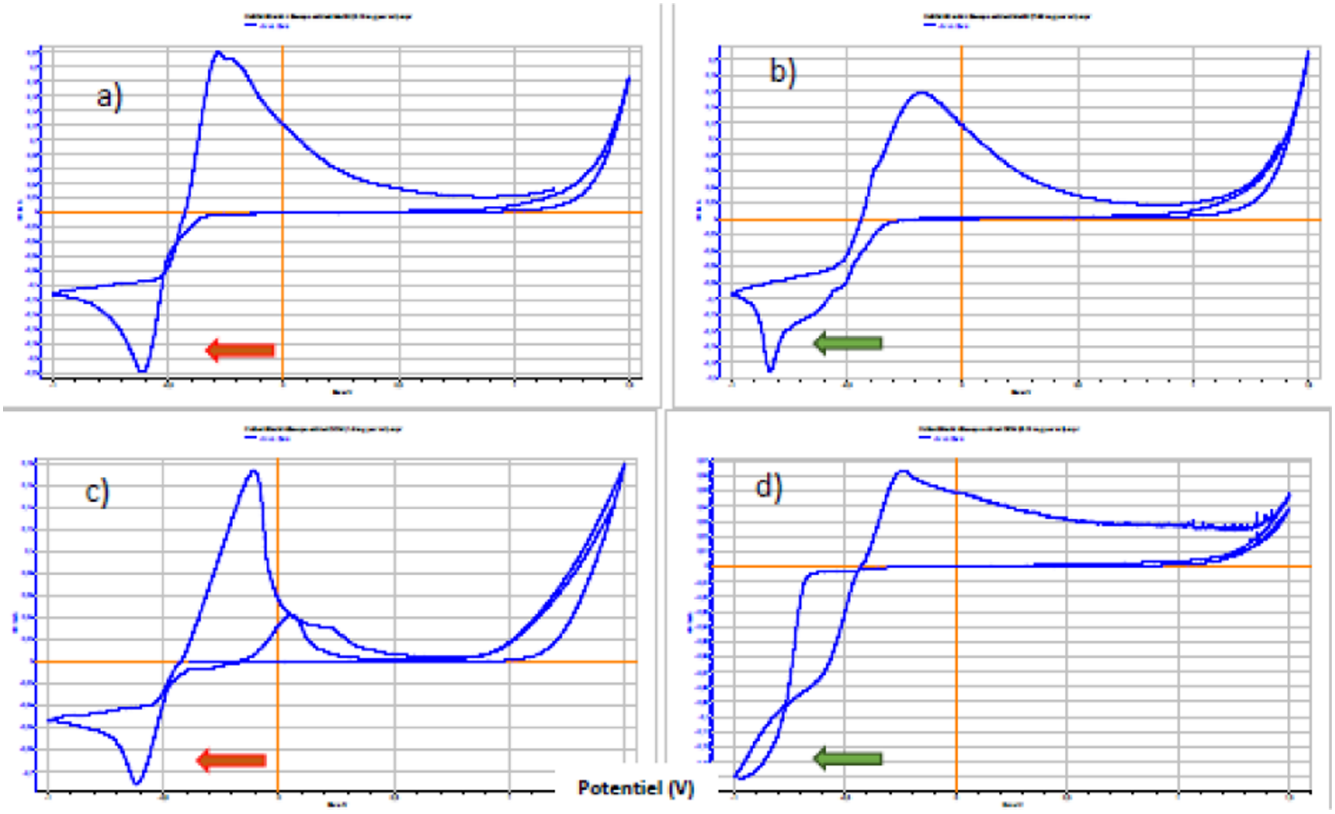

Figure 6. Cyclic voltammograms of solutions of (a) $CuSO_4$ [50 mM] + methanolic extract of *B. monnieri* (3.19 mg/mL), (b) $CuSO_4$ [50 mM] + methanolic extract of *B. monnieri* (7.98 mg/mL), (c) $CuSO_4$ [50 mM] + dichloromethane extract of *B. monnieri* (1.16 mg/mL), and (d) $CuSO_4$ [50 mM] + dichloromethane extract of *B. monnieri* (3.19 mg/mL), in phosphate buffer 0.10 M, pH 7.0. Potential scan rate: 20 mV s^{-1}.

second strains allow us to investigate how a substance may be neuroprotective[25] (see below). Analysis of the 40Q worms, treated with different Bacopa extracts, showed that this plant contains chemicals with the power to reduce polyQ aggregation (Figure 7). For example, treating the worms with the *B. monnieri* extracts (whole plant), obtained with DCM, reduces the rate of aggregation from 30 inclusion bodies (30.9 ± 0.8, average ± SEM), in the control worms treated with the vehicle (DMSO), compared to 13 (13.5 ± 1.3) in the worms treated with the extract ($p < 0.001$) (Figure 7A). The rest of extracts, obtained with DCM, followed the same trend of reduction of aggregation of polyQs, but there were substantial differences depending on the part of the plant being tested. While the whole plant extract reduced massively the number of inclusion bodies (13.5 ± 1.3), the extract obtained just with the leaves did not, at least not to the same extent (25.3 ± 1.3) (Figure 7A). The root extract, in contrast, reduced substantially the aggregation process ($p < 0.001$) (16.5 ± 1.6) (Figure 7A). Since reduction from the whole plan extract and reduction from the root part are not statistically different, we may assume that the most active compound is in the root of Bacopa plants, although the leaves seem to have also protective substances. With regard to MeOH extracts of Bacopa, the trend is similar to the results obtained with DCM extracts. The whole plant MeOH extract reduced the inclusion bodies to 12.7 ± 1.6, which is not statistically different to the effect observed with the treatment with the DCM extract (13.5 ± 1.3) (Figure 7A). Interestingly, both leaves and roots show the same level of reduction of aggregation patterns (18.7 ± 1.2 and 20.0 ± 1.6 respectively) (Figure 7A). This result is substantially softer than the reduction observed with the whole extract (12.7 ± 1.6) ($p < 0.001$), which suggests that different species from both plant parts may act together to reduce the formation of inclusion bodies of polyQs in *C. elegans* (Figure 7A). Both methods to produce the Bacopa extracts seem to provide with functional bacosides since both kind of extracts reduces polyQ aggregation in worms. In this regard, it has been shown that hexane-produced Bacopa extracts provided with products that enhanced the lifespan, by reducing oxidative stress caused by glutamate toxicity in worm murine models.[42−44] With regard to the reduction of polyQ aggregation and polyQ-induced stress, it has been shown that bacosides were able to induce chaperone expression in rats and also promote anti-oxidative molecules.[45]

Analysis of Neuroprotective Activity in *C. elegans* Neurons Stressed with polyQs. The above results are interesting, from the mechanistical point of view, because it does suggest that these extracts may act in favor of protein homeostasis. However, we wanted to investigate whether they have an effect on functional matters. To do so, we studied the effect of these extracts on neurons stressed with polyQs. Hence, we incubated the 112Q strain in the same conditions described above and then assayed for the touch response. Typically, the 112Q animals respond around 20−25% of the times that they are touched with an eyelash mounted on a toothpick[24] because the touch receptor neurons are stressed with the polyQs. However, analysis of the touch response of the animals grown on Bacopa shows that these extracts are able to partially restore the functionality on these neurons (Figure 7B). For example, 112Q worms grown on DCM-produced Bacopa extract increased up to 50% more than their capacity of mechanosensation (Figure 7B) (from 18.9% ± 0.6 to 30.3% ±

https://doi.org/10.1021/acsomega.1c03378
ACS Omega 2022, 7, 16260−16269

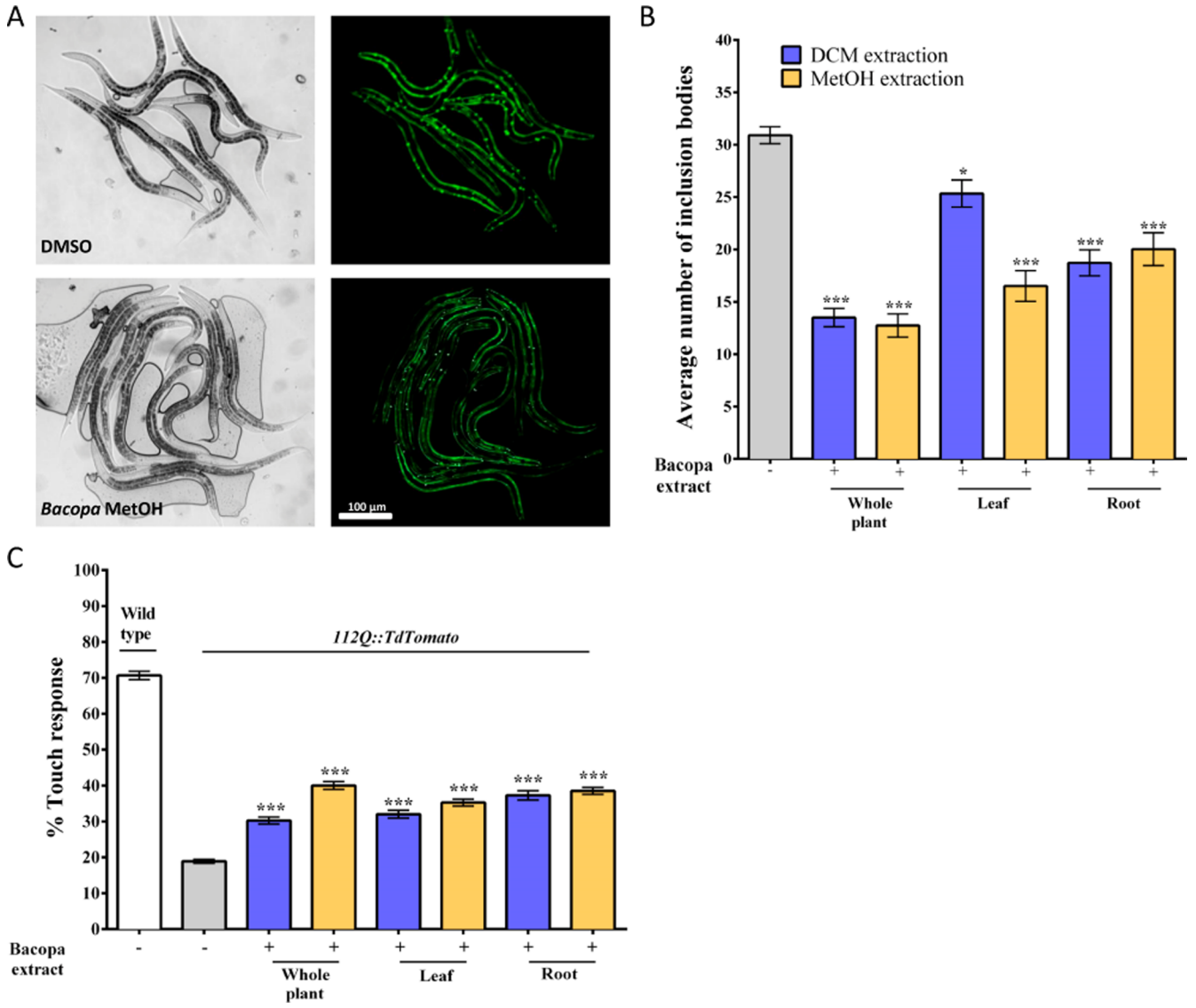

Figure 7. Bacoside extracts protect *C. elegans* from polyQ-induced toxicity and restores the neuronal function. (A) Transmission and fluorescent microscopy images from worms expressing 40Q::YFP in body wall muscles, treated with MetOH extract of Bacopa (below), and their respective control with DMSO (above); (B) quantification of the aggregation phenotype, from worms treated with different extracts from different parts of the Bacopa plants and also different methods of extraction. Bacosides reduce substantially the aggregation phenotype of worms; (C) Bacosides are able to induce neuroprotection in worms stressed by polyQs (112Q::tdTomato expressed in mechanosensory neurons). Asterisk show statistical significance from the ANOVA test with Tukey posthoc: $*p < 0.05$; $***p < 0.001$.

1.0, $p < 0.001$). The DCM extracts from leaves and roots also restored the mechanosensation of the 112Q worms, raising the touch response substantially, from 18.9 ± 0.6 of the worms treated with the vehicle (DMSO) to 32.0% ± 1.1 ($p < 0.001$) and 35.3% ± 1.0 ($p < 0.001$), respectively (Figure 7B). Interestingly, the extracts obtained with the MeOH method resulted slightly better in rescuing the touch phenotype. The whole plant extract, for example, rescued worms from 18.9% ± 0.6 to 40% ± 1.1 ($p < 0.001$) (Figure 7B). The results obtained with leaf and root extracts resulted in very similar effects 37.3% ± 1.3 and 38.5% ± 1.0, respectively. Both were statistically significant and different from controls but not substantially different from the MeOH extract of the whole plant. This suggests that both tissues contain similar protective compounds and probably at similar concentrations. These neuroprotective effects have been shown in murine models of Parkinson disease, a pathology that shares many traits with HD.[46] Moreover, these extracts also reduce phenotypes in the models of epilepsy in worms[47] and rats.[48]

■ CONCLUSIONS

Spectroscopic and electrochemical screening of molecules and plant extracts with neuroprotective activity, through the cooper-binding mechanism, can be performed, in aqueous media at biological pH, using voltammetry of microparticles. Electrodes are modified with microparticulate films of the tested compounds and immersed into Cu^{2+} solutions. In all cases, the voltammetric signals of Cu^{2+} exhibit significant peak splitting in the presence of compounds interacting significantly with copper. Peak splitting observed in voltammetric peaks for electrodes modified with compounds displaying neuroprotective activity can be interpreted on the basis of a Hess' cycle process involving surface-confined complexes. The described solid-state electrochemistry screening provides high sensitivity

https://doi.org/10.1021/acsomega.1c03378
ACS Omega 2022, 7, 16260−16269

with the amounts of compound to be tested in the microgram−nanogram range. This methodology is particularly interesting because it opens the possibility of testing cooper−ligand interactions in the aqueous environment at physiological pH, with no need of previous incubation, and it can be used at the nanoscopic level. Using this technology, we were able to test Bacopa extracts, which showed great ability to chelate copper ions. This, together with the literature about Bacopa and the neurodegenerative diseases field, strongly pointed out that the extracts may be of interest to reduce phenotypes in the animal models of HD. As we hypothesized, these compounds were able to reduce the aggregation of polyQ-containing proteins in *C. elegans* worms expressing these toxic molecules in muscle cells. However, the reduction of aggregation does not always parallel the recovery of function. Hence, we tested these extracts into a worm model of neuronal toxicity. Interestingly, these extracts are able to restore neuronal function of worms with mechanosensory neurons challenged by polyQs. Proteins containing abnormal expansions of CAG, hence encoding long tracks of polyQs are causative of a number neurodegenerative diseases, including HD, spinocerebellar ataxias, and a few more, which to date are orphan of a treatment. Our findings places Bacopa as a new player to fight neurodegenerative disorders, caused by prone-to-aggregation proteins.

MATERIALS AND METHODS

A library of compounds employed in this study was composed of two different groups of molecules (Chart 1): (a) organic molecules with copper(II)-chelating properties: ethylenediaminetetraacetic acid (EDTA),[24] phenylenediamine (PPD), and extracts of *B. monnieri* (dichloromethane [DCM] and methanol [MeOH]) and (b) active molecules against neurodegenerative diseases involving or not involving Cu-binding: metformin (MET),[25] salicylate (SAL),[26,27] and trehalose (TRE).[28]

Chart 1. Chemical Structures Employed in This Work: EDTA, PPD, Bacoside A, a Major Constituent of *B. monnieri*, MET, SAL and TRE

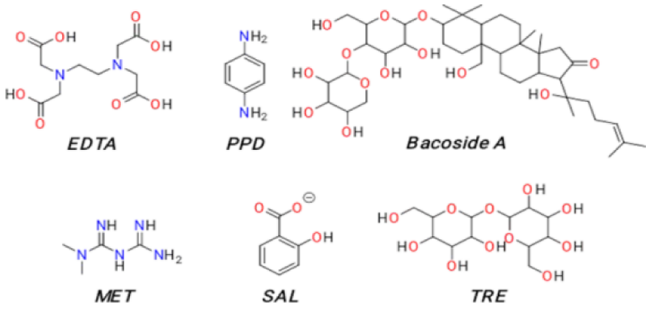

Collection and Treatment of the Plant Material. *B. monnieri* L. (Figure 1) was collected on March 21, 2019 at "*La maison de la mangrove*", in the commune of Abymes (Guadeloupe, France). The plant was immediately cleaned with distilled water and dried three weeks in the ambient air before being crushed.

Extraction of the Plant Material by Soxhlet. *B. monnieri* is composed of different triterpenoid saponins, known as bacosides; bacoside A is its major constituent.[23] For the extraction, pumice stones were introduced to regulate the boiling in a 1 L glass flask previously weighted. A cellulose cartridge containing 51.24 g of plant material (*B. monnieri*) was introduced into the glass body of the Soxhlet extractor. Then, the cartridge was impregnated with 600 mL of dichloromethane. The extraction was carried out for 48 h. After the extraction, the solvent was dry evaporated using a rotary evaporator, obtaining 1.2 g (yield of 2.4%) of product. The cartridge underwent a second extraction cycle with 600 mL of methanol for 48 h. Then, the solvent was totally evaporated using a rotary evaporator, and 12.4 g of product was obtained (yield: 24.2%).

UV−Vis Spectroscopy Experiments. A PerkinElmer brand spectrophotometer was used to define the λ_{max} of $CuSO_4$ (~800 nm) and analyze the solutions. The λ_{max} of different solutions has been studied by scanning a predefined wavelength range. For these experiments, several molecules (EDTA, PPD, MET, SAL, TRE, and the extracts of *B. monnieri* in DCM and MeOH) have been analyzed according to their ability to chelate the metal ion Cu^{2+}. 50 mM of $CuSO_4$ solution (pH ≈ 7.0) was added in each solution, and increasing amounts of EDTA (10 to 200 mM), PPD (10 to 40 mM), MET, SAL, or TRE (10, 20 and 50 mM) was added. For experiments using the extracts of *B. monnieri*, copper solutions were prepared by adding increasing amounts of dry extracts.

Electrochemical Experiments. Solution-phase electrochemical experiments were performed on a glassy carbon electrode at 298 ± 1 K using conventional equipment. The solutions of different molecules (EDTA, PPD, MET, TRE, and SAL) previously prepared to develop the spectroscopic experiments were used to study the electrochemical profile of Cu^{2+}. For these experiments, phosphate buffer, 0.10 M pH 7.0, was added in each solution, at a ratio of 8:2 (8 mL of solution to be analyzed + 2 mL of buffer), and a $CuSO_4$ solution 50 mM was employed.

***C. elegans* Strains.** *C. elegans* nematode was maintained at 20 °C as previously described by Brenner.[29] AM141 and RVM131 strains were used to evaluate the protective effect in muscle cells and neurons of *B. monnieri* L., respectively. AM141 contains a transgene that express 40 glutamines (40Q) in frame with the fluorescent protein YFP in muscle cells with genotype *rmIs133[unc-54p::40Q::YFP]*.[30] This strain was provided by the Caenorhabditis Genetics Center (University of Minnesota, Minnesota, USA). The transgene included in RVM131 animals drives the expression of 112Q fused to the fluorescent protein tandem tomato (TdTomato) in mechanosensory neurons (genotype *vltEx131[mec-3p::112Q::TdTomato; myo-2p::GFP]*).[25]

***C. elegans* Maintenance and Culture.** The nematode growth medium (NGM) was used in order to grow and culture the worms.[29] NGM was prepared with 3 g of NaCl, 20 g of bacteriological agar, and 2.5 g of peptone in 1 L of H_2O. After autoclaving, the NGM medium was supplemented with cholesterol (5 mg/mL in ethanol), nystatin suspension (12.5 mg/mL), 1 mL of $CaCl_2$ 1 M, 1 mL of $MgSO_4$ 1 M, and 25 mL of KH_2PO_4 1 M, pH 6.0. The medium was immediately poured into plates (10 mL/well). After drying in an extractor with laminar flow, the plates were seeded with the OP50 *Escherichia coli* strain and also dried. For the amplification, the nematodes were transplanted from one Petri dish after 72 h. Then, the selection of plates was based on those that contain hermaphrodites carrying eggs. The selected plates were washed with few milliliters of M9 buffer medium and collected in falcon 15 mL centrifuge tubes. Then, a standard bleaching

https://doi.org/10.1021/acsomega.1c03378
ACS Omega 2022, 7, 16260−16269

buffer was performed according to Porta-de-la-Riva et al.[31] with modifications. The tubes were centrifuged to 20 °C at 1500 rpm during 1 min, and the supernatant was removed. The mixture was prepared by adding 250 μL of H_2O, 0.5 mL of commercial bleach solution (4−6% hypochlorite), and 1.25 mL of NaOH, in water. The solution was shacked during 5−6 min on a vortex, the supernatant was removed, and 15 mL of M9 buffer medium (1×) was added. M9 buffer is a physiological buffer consisting of 3 g of KH_2PO_4, 6 g of Na_2HPO_4, and 5 g of NaCl in 1 L of H_2O, and then, after autoclaving it, 1 mL of $MgSO_4$ 1 M was added. This operation was repeated but leaving 1 mL of supernatant. The worms were suspended before incubation at 20 °C in agitation for 24 h for the embryos to hatch. Then, the larvae were left in the physiological solution without food to synchronize to the L1 stage. Then, L1 animals were incubated with different plant extracts, using microplates of 96 wells with a capacity of 100 μL, during 72 h at 20 °C on a wet atmosphere and agitated. L4 and young adults were evaluated by counting the number of inclusion bodies and mechanosensory response, respectively. The experiments were reproduced at least three times. Manual isolation of stage L4 nematodes was performed using a tin wire soldered to a glass Pasteur pipette, allowing the worms to be gently handled, as described elsewhere[25,32] under a dissecting microscope equipped with fluorescence (Leica M165 FC, Leica Microsystems, Wetzlar, Germany).

Analysis of polyQ Aggregation. The average number of inclusion bodies in muscle cells was analyzed under a dissecting microscope equipped with fluorescence (Leica M165 FC). To analyze aggregation, we observed AM141 worms under a microscope, since these proteins collapse into inclusion bodies. We counted in vivo the number of these inclusion bodies, from at least 30 L4 larvae, per treatment. Then an average was calculated and plotted into graphs.

Touch Assays. Touch assays were performed by gently passing an eyelash, mounted on a toothpick, through the tail of the worms, as described elsewhere.[25,32] The tail of each worm was scored approximately 10 times. This test was performed on approximately 50 animals, and the average response was plotted. Each assay was repeated at least three independent times.

Statistical Analyses. Statistical analyses were performed in GraphPad Prism by subjecting the data to one-way ANOVA, followed by the Tukey multiple comparison test as can be seen in other similar studies.[25,32] The results are presented as means ± SEM (standard error of the mean) of the mean number of inclusion bodies in muscle cells by a nematode. Then, they were compared to nematodes treated only with DMSO (0.0025%) in the control.

AUTHOR INFORMATION

Corresponding Authors

Rafael P. Vázquez-Manrique − *Laboratory of Molecular, Cellular and Genomic Biomedicine, Instituto de Investigación Sanitaria La Fe, Valencia 46026, Spain; Joint Unit for Rare Diseases IIS La Fe-CIPF, Valencia 46012, Spain; Centro de Investigación Biomédica en Red de Enfermedades Raras (CIBERER), Madrid 46010, Spain;* orcid.org/0000-0002-1594-0033; Email: rafael_vazquez@iislafe.es

Gerardo Cebrián-Torrejón − *COVACHIM-M2E Laboratory EA 3592, UFR SEN, Department of Chemistry, University of the French West Indies, Pointe-à-Pitre Cedex 97157, France;* orcid.org/0000-0002-5776-922X; Email: gerardo.cebrian-torrejon@univ-antilles.fr

Authors

David Brinvillier − *COVACHIM-M2E Laboratory EA 3592, UFR SEN, Department of Chemistry, University of the French West Indies, Pointe-à-Pitre Cedex 97157, France*

Melissa Barrast − *COVACHIM-M2E Laboratory EA 3592, UFR SEN, Department of Chemistry, University of the French West Indies, Pointe-à-Pitre Cedex 97157, France*

Petra Couderc-Murillo − *COVACHIM-M2E Laboratory EA 3592, UFR SEN, Department of Chemistry, University of the French West Indies, Pointe-à-Pitre Cedex 97157, France; UA, UMR EcoFoG, CNRS, Cirad, INRA, Université des Antilles, Université de Guyane, Université des Antilles, Pointe-à-Pitre 97159, France;* orcid.org/0000-0001-9965-3439

José Bono-Yagüe − *Laboratory of Molecular, Cellular and Genomic Biomedicine, Instituto de Investigación Sanitaria La Fe, Valencia 46026, Spain; Joint Unit for Rare Diseases IIS La Fe-CIPF, Valencia 46012, Spain*

Alain Rousteau − *UA, UMR EcoFoG, CNRS, Cirad, INRA, Université des Antilles, Université de Guyane, Université des Antilles, Pointe-à-Pitre 97159, France*

Ana Pilar Gómez Escribano − *Laboratory of Molecular, Cellular and Genomic Biomedicine, Instituto de Investigación Sanitaria La Fe, Valencia 46026, Spain; Joint Unit for Rare Diseases IIS La Fe-CIPF, Valencia 46012, Spain; Centro de Investigación Biomédica en Red de Enfermedades Raras (CIBERER), Madrid 46010, Spain*

Marcos V. Palmeira-Mello − *Instituto de Química, Universidade Federal Fluminense, Niterói 24020-141 RJ, Brazil;* orcid.org/0000-0003-2550-5315

Antonio Doménech-Carbó − *Departament de Química Analítica, Facultat de Química, Universitat de València, Burjassot 46100 Valencia, Spain;* orcid.org/0000-0002-5284-2811

Nady Passe-Coutrin − *COVACHIM-M2E Laboratory EA 3592, UFR SEN, Department of Chemistry, University of the French West Indies, Pointe-à-Pitre Cedex 97157, France*

Muriel Sylvestre − *COVACHIM-M2E Laboratory EA 3592, UFR SEN, Department of Chemistry, University of the French West Indies, Pointe-à-Pitre Cedex 97157, France*

Complete contact information is available at: https://pubs.acs.org/10.1021/acsomega.1c03378

Author Contributions

The manuscript was written through contributions of all authors. All authors have given approval to the final version of the manuscript.

Notes

The authors declare no competing financial interest.

ACKNOWLEDGMENTS

This study was supported by the European Union Fund (FEDER) in the framework of AgroEcoDiv project. We wish to thank the CGC (funded by NIH Office of Research Infrastructure Programs; ref: P40 OD010440). We also thank AVAEH, the Valencian Association of the Huntington Disease, for funding part of this work. RPVM was a Miguel Servet type II researcher (CPII16/00004) ISCIII. Grants from the ISCIII partially fund the laboratory of RVM (PI17/00011 and PI20/00114). This work has been partially supported by a grant

https://doi.org/10.1021/acsomega.1c03378
ACS Omega 2022, 7, 16260−16269

from Fundación Ramón Areces (CIVP19S8119) and an Ayuda Miguel Gil grant to RPVM (VII Convocatoria Ayudas a la Investigación MHER, 2019, cofinanced by Colegio Oficial de Farmacéuticos de Sevilla and Fundación Cajasol). All grants from ISCIII are cofinanced by the European Development Regional Fund "A way to achieve Europe" (ERDF). Some equipment used in this work have been funded in partnership between the Generalitat Valenciana (Conselleria de Sanitat I Salut Pública, Valencian Community, Spain) and ERDF.

REFERENCES

(1) Roos, R. A. Huntington's disease: a clinical review. *Orphanet J. Rare Dis.* **2010**, *5*, 40.
(2) Bono-Yagüe, J.; Gómez-Escribano, A. P.; Millán, J. M.; Vázquez-Manrique, R. P. Reactive Species in Huntington Disease: Are They Really the Radicals You Want to Catch? *Antioxidants* **2020**, *9*, 577.
(3) Pan, L.; Feigin, A. Huntington's Disease: New Frontiers in Therapeutics. *Curr. Neurol. Neurosci. Rep.* **2021**, *21*, 10.
(4) Fox, J. H.; Kama, J. A.; Lieberman, G.; Chopra, R.; Dorsey, K.; Chopra, V.; Volitakis, I.; Cherny, R. A.; Bush, A. I.; Hersch, S. Mechanisms of Copper Ion Mediated Huntington's Disease Progression. *PLoS One* **2007**, *2*, No. e334.
(5) Kozlowski, H.; Luczkowski, M.; Remelli, M.; Valensin, D. Copper, zinc and iron in neurodegenerative diseases (Alzheimer's, Parkinson's and prion diseases). *Coord. Chem. Rev.* **2012**, *256*, 2129.
(6) Festa, R. A.; Thiele, D. J. Copper: an Essential Metal in Biology. *Curr. Biol.* **2011**, *21*, R877.
(7) Duncan, C.; White, A. R. Copper complexes as therapeutic agents. *Metallomics* **2012**, *4*, 127.
(8) Krasnovskaya, O.; Naumov, A.; Guk, D.; Gorelkin, P.; Erofeev, A.; Beloglazkina, E.; Majouga, A. Copper Coordination Compounds as Biologically Active Agents. *Int. J. Mol. Sci.* **2020**, *21*, 3965.
(9) Palmeira-Mello, M. V.; Caballero, A. B.; Lopez-Espinar, A.; Guedes, G. P.; Caubet, A.; de Souza, A. M. T.; Lanznaster, M.; Gamez, P. DNA-interacting properties of two analogous square-planar cis-chlorido complexes: copper versus palladium. *J. Biol. Inorg Chem.* **2021**, *26*, 727.
(10) Suntharalingam, K.; Hunt, D. J.; Duarte, A. A.; White, A. J. P.; Mann, D. J.; Vilar, R. A Tri-copper(II) Complex Displaying DNA-Cleaving Properties and Antiproliferative Activity against Cancer Cells. *Chem.—Eur. J.* **2012**, *18*, 15133.
(11) Rivera-Mancía, S.; Pérez-Neri, I.; Ríos, C.; Tristán-López, L.; Rivera-Espinosa, L.; Montes, S. The transition metals copper and iron in neurodegenerative diseases. *Chem.-Biol. Interact.* **2010**, *186*, 184.
(12) Gil-Mohapel, J.; Brocardo, P.; Christie, B. The role of oxidative stress in Huntington's disease: are antioxidants good therapeutic candidates? *Curr. Drug Targets* **2014**, *15*, 454.
(13) Huang, X.; Li, N.; Pu, Y.; Zhang, T.; Wang, B. Neuroprotective Effects of Ginseng Phytochemicals: Recent Perspectives. *Molecules* **2019**, *24*, 2939.
(14) Martínez-Coria, H.; Mendoza-Rojas, M. X.; Arrieta-Cruz, I.; López-Valdés, H. E. Preclinical Research of Dihydromyricetin for Brain Aging and Neurodegenerative Diseases. *Front. Pharmacol.* **2019**, *10*, 1334.
(15) Rajabian, A.; Sadeghnia, H.; Fanoudi, S.; Hosseini, A. Genus Boswellia as a new candidate for neurodegenerative disorders. *Iran. J. Basic Med. Sci.* **2020**, *23*, 277.
(16) Razavi, S. M.; Khayatan, D.; Arab, Z. N.; Momtaz, S.; Zare, K.; Jafari, R. M.; Dehpour, A. R.; Abdolghaffari, A. H. Licofelone, a potent COX/5-LOX inhibitor and a novel option for treatment of neurological disorders. *Prostaglandins Other Lipid Mediators* **2021**, *157*, 106587.
(17) Pagano, K.; Tomaselli, S.; Molinari, H.; Ragona, L. Natural Compounds as Inhibitors of Aβ Peptide Aggregation: Chemical Requirements and Molecular Mechanisms. *Front. Neurosci.* **2020**, *14*, 619667.
(18) Lakey-Beitia, J.; Burillo, A. M.; La Penna, G.; Hegde, M. L.; Rao, K. S. Polyphenols as Potential Metal Chelation Compounds Against Alzheimer's Disease. *J. Alzheimer's Dis.* **2021**, *82*, S335.
(19) Picciano, A. L.; Vaden, T. D. Complexation between Cu(II) and curcumin in the presence of two different segments of amyloid β. *Biophys. Chem.* **2013**, *184*, 62.
(20) Kola, A.; Hecel, A.; Lamponi, S.; Valensin, D. Novel Perspective on Alzheimer's Disease Treatment: Rosmarinic Acid Molecular Interplay with Copper(II) and Amyloid β. *Life* **2020**, *10*, 118.
(21) Mukherjee, S.; Dugad, S.; Bhandare, R.; Pawar, N.; Jagtap, S.; Pawar, P.K.; Kulkarni, O. Evaluation of comparative free-radical quenching potential of Brahmi (Bacopamonnieri) and Mandookparni (Centellaasiatica). *AYU* **2011**, *32*, 258.
(22) Russo, A.; Borrelli, F. Bacopa monniera, a reputed nootropic plant: an overview. *Phytomedicine* **2005**, *12*, 305.
(23) Sekhar, V. C.; Viswanathan, G.; Baby, S. Insights into the Molecular Aspects of Neuroprotective Bacoside A and Bacopaside I. *Curr. Neuropharmacol.* **2019**, *17*, 438.
(24) Inoue, F.; Philipsen, H.; Radisic, A.; Armini, S.; Civale, Y.; Shingubara, S.; Leunissen, P. Electroless Copper Bath Stability Monitoring with UV-VIS Spectroscopy, pH, and Mixed Potential Measurements. *J. Electrochem. Soc.* **2012**, *159*, D437.
(25) Sanchis, A.; García-Gimeno, M. A.; Cañada-Martínez, A. J.; Sequedo, M. D.; Millán, J. M.; Sanz, P.; Vázquez-Manrique, R. P. Metformin treatment reduces motor and neuropsychiatric phenotypes in the zQ175 mouse model of Huntington disease. *Exp. Mol. Med.* **2019**, *51*, 1.
(26) Markowicz-Piasecka, M.; Sikora, J.; Szydłowska, A.; Skupień, A.; Mikiciuk-Olasik, E.; Huttunen, K. M. Metformin - a Future Therapy for Neurodegenerative Diseases. *Pharm. Res.* **2017**, *34*, 2614.
(27) Pomponi, M.; Pomponi, M. F. L. Alzheimer's disease prevention & acetyl salicylic acid: a believable story. *Indian J. Med. Res.* **2014**, *139*, 1−3.
(28) Du, J.; Liang, Y.; Xu, F.; Sun, B.; Wang, Z. Trehalose rescues Alzheimer's disease phenotypes in APP/PS1 transgenic mice: Trehalose rescues Alzheimer's disease phenotypes. *J. Pharm. Pharmacol.* **2013**, *65*, 1753.
(29) Brenner, S. The Genetics of Caenorhabditis Elegans. *Genetics* **1974**, *77*, 71−94.
(30) Morley, J. F.; Brignull, H. R.; Weyers, J. J.; Morimoto, R. I. The threshold for polyglutamine-expansion protein aggregation and cellular toxicity is dynamic and influenced by aging in Caenorhabditis elegans. *Proc. Natl. Acad. Sci. U.S.A.* **2002**, *99*, 10417.
(31) Porta-de-la-Riva, M.; Fontrodona, L.; Villanueva, A.; Cerón, J. Basic Caenorhabditis elegans methods: synchronization and observation. *J. Visualized Exp.* **2012**, *64*, No. e4019.
(32) Gómez-Escribano, A.; Bono-Yagüe, J.; García-Gimeno, M.; Sequedo, M.; Hervás, D.; Fornés-Ferrer, V.; Torres-Sánchez, S.; Millán, J.; Sanz, P.; Vázquez-Manrique, R. Synergistic activation of AMPK prevents from polyglutamine-induced toxicity in Caenorhabditis elegans. *Pharmacol. Res.* **2020**, *161*, 105105.
(33) Kucková, L.; Jomová, K.; Švorcová, A.; Valko, M.; Segla, P.; Moncol, J.; Kožíšek, J. Synthesis, Crystal Structure, Spectroscopic Properties and Potential Biological Activities of Salicylate−Neocuproine Ternary Copper(II) Complexes. *Molecules* **2015**, *20*, 2115.
(34) Mondal, B.; Kumar, P.; Ghosh, P.; Kalita, A. Fluorescence-based detection of nitric oxide in aqueous and methanol media using a copper(II) complex. *Chem. Commun.* **2011**, *47*, 2964.
(35) Anderson, J. L.; Shain, I. Cyclic Voltammetric Studies of Ionic Strength and Nitrate Ion Dependence of Copper(II) Reduction in Acidic Aqueous Nitrate and Perchlorate Solutions. *Anal. Chem.* **1978**, *50*, 163.
(36) Abdul Manap, A. S.; Vijayabalan, S.; Madhavan, P.; Chia, Y. Y.; Arya, A.; Wong, E. H.; Rizwan, F.; Bindal, U.; Koshy, S. Bacopa monnieri, a Neuroprotective Lead in Alzheimer Disease: A Review on Its Properties, Mechanisms of Action, and Preclinical and Clinical Studies. *Drug Target Insights* **2019**, *13*, 117739281986641.

https://doi.org/10.1021/acsomega.1c03378
ACS Omega 2022, 7, 16260−16269

(37) Jyoti, A.; Sharma, D. Neuroprotective role of Bacopa monniera extract against aluminium-induced oxidative stress in the hippocampus of rat brain. *Neurotoxicology* **2006**, *27*, 451.
(38) Yeung, A. W. K.; Tzvetkov, N. T.; Georgieva, M. G.; Ognyanov, I. V.; Kordos, K.; Jóźwik, A.; Kühl, T.; Perry, G.; Petralia, M. C.; Mazzon, E.; Atanasov, A. G. Reactive Oxygen Species and Their Impact in Neurodegenerative Diseases: Literature Landscape Analysis. *Antioxid. Redox Signaling* **2021**, *34*, 402.
(39) Parker, J. A.; Connolly, J. B.; Wellington, C.; Hayden, M.; Dausset, J.; Neri, C. Expanded polyglutamines in Caenorhabditis elegans cause axonal abnormalities and severe dysfunction of PLM mechanosensory neurons without cell death. *Proc. Natl. Acad. Sci. U.S.A.* **2001**, *98*, 13318.
(40) Vázquez-Manrique, R. P.; Farina, F.; Cambon, K.; Dolores Sequedo, M.; Parker, A. J.; Millán, J. M.; Weiss, A.; Déglon, N.; Neri, C. AMPK activation protects from neuronal dysfunction and vulnerability across nematode, cellular and mouse models of Huntington's disease. *Hum. Mol. Genet.* **2016**, *25*, 1043.
(41) Arrasate, M.; Finkbeiner, S. Protein aggregates in Huntington's disease. *Exp. Neurol.* **2012**, *238*, 1.
(42) Brimson, J. M.; Prasanth, M. I.; Plaingam, W.; Tencomnao, T. Bacopa monnieri (L.) wettst. Extract protects against glutamate toxicity and increases the longevity of Caenorhabditis elegans. *Afr. J. Tradit., Complementary Altern. Med.* **2020**, *10*, 460.
(43) Pandey, R.; Phulara, S.; Shukla, V.; Tiwari, S. Bacopa monnieri promotes longevity in Caenorhabditis elegans under stress conditions. *Pharmacogn. Mag.* **2015**, *11*, 410.
(44) Bhattacharya, S. K.; Bhattacharya, A.; Kumar, A.; Ghosal, S. Antioxidant activity of Bacopa monnieri in rat frontal cortex, striatum and hippocampus. *Phytother. Res.* **2000**, *14*, 174.
(45) Chowdhuri, D. K.; Parmar, D.; Kakkar, P.; Shukla, R.; Seth, P. K.; Srimal, R. C. Antistress effects of bacosides of Bacopa monnieri: modulation of Hsp70 expression, superoxide dismutase and cytochrome P450 activity in rat brain. *Phytother. Res.* **2002**, *16*, 639.
(46) Singh, B.; Pandey, S.; Rumman, M.; Kumar, S.; Kushwaha, P. P.; Verma, R.; Mahdi, A. A. Neuroprotective and Neurorescue Mode of Action of Bacopa monnieri (L.) Wettst in 1-Methyl-4-phenyl-1,2,3,6-tetrahydropyridine-Induced Parkinson's Disease: An In Silico and In Vivo Study. *Front. Pharmacol.* **2021**, *12*, 616413.
(47) Pandey, R.; Gupta, S.; Tandon, S.; Wolkenhauer, O.; Vera, J.; Gupta, S. K. Baccoside A suppresses epileptic-like seizure/convulsion in Caenorhabditis elegans. *Seizure* **2010**, *19*, 439.
(48) Komali, E.; Venkataramaiah, C.; Rajendra, W. Antiepileptic potential of Bacopa monnieri in the rat brain during PTZ-induced epilepsy with reference to cholinergic system and ATPases. *Afr. J. Tradit., Complementary Altern. Med.* **2021**, *11*, 137.

https://doi.org/10.1021/acsomega.1c03378
ACS Omega 2022, 7, 16260−16269